HHS Public Access

Author manuscript

Free Radic Biol Med. Author manuscript; available in PMC 2017 May 01.

Published in final edited form as:

Free Radic Biol Med. 2016 May ; 94: 161–173. doi:10.1016/j.freeradbiomed.2016.01.020.

Distinct oxidative cleavage and modification of bovine [Cu-Zn]-SOD by an ascorbic acid/Cu(II) system: Identification of novel copper binding site on SOD molecule

Hiroshi Uehara[a], **Shen Luo**[a], **Baikuntha Aryal**[a], **Rodney L. Levine**[b], and **V. Ashutosh Rao**[a,*]

[a]Laboratory of Applied Biochemistry, Division of Biotechnology Review and Research III, Office of Biotechnology Products, Center for Drug Evaluation and Research, Food and Drug Administration, White Oak, MD 20993, USA

[b]Laboratory of Biochemistry, National Heart, Lung, and Blood Institute, Bethesda, MD 20892, USA

Abstract

We investigated the combined effect of ascorbate and copper [Asc/Cu(II)] on the integrity of bovine [Cu-Zn]-superoxide dismutase (bSOD1) as a model system to study the metal catalyzed oxidation (MCO) and fragmentation of proteins. We found Asc/Cu(II) mediates specific cleavage of bSOD1 and generates 12.5 and 3.2 kDa fragments in addition to oxidation/carbonylation of the protein. The effect of other tested transition metals, a metal chelator, and hydrogen peroxide on the cleavage and oxidation indicated that binding of copper to a previously unknown site on SOD1 is responsible for the Asc/Cu(II) specific cleavage and oxidation. We utilized tandem mass spectrometry to identify the specific cleavage sites of Asc/Cu(II)-treated bSOD1. Analyses of tryptic- and AspN-peptides have demonstrated the cleavage to occur at Gly31 with peptide bond breakage with Thr30 and Ser32 through diamide and α-amidation pathways, respectively. The three-dimensional structure of bSOD1 reveals the imidazole ring of His19 localized within 5 Angstrom from the α-carbon of Gly31 providing a structural basis that copper ion, most likely coordinated by His19, catalyzes the specific cleavage reaction.

Keywords

SOD; metal catalyzed oxidation; copper; ascorbic acid; carbonylation; mass spectrometry

*To whom correspondence should be addressed: Ashutosh Rao, Office of Biotechnology roducts, Center for Drug Evaluation and Research, Food and Drug Administration, 10903 New Hampshire Avenue, Rm 2212, Silver Spring, MD 20993, USA, Tel.: 240-402-7338; Fax: (301) 480-3256; ashutosh.rao@fda.hhs.gov.

Disclosures:

The authors have no competing financial interests to disclose. The views expressed in this article are those of the authors and do not necessarily reflect the official policy or position of the U.S. Food and Drug Administration and the Department of Health and Human Services, nor does mention of trade names, commercial products, or organizations imply endorsement by the U.S. Government.

Introduction

The metal catalyzed oxidation (MCO) of proteins introduces carbonyl moieties into protein side chains, and under certain conditions, causes fragmentation of the protein. MCOs have been proposed to play a role in oxidative stress, disease and aging (1,2). *In vivo*, protein carbonylation has often been utilized as a hallmark of ROS-mediated protein oxidation as the carbonyl modifications are irreversible and are introduced directly by MCO or indirectly through lipid peroxidation or advanced glycation end products pathways (3–8). *In vitro*, therapeutic proteins are prone to oxidative modification during manufacturing, processing, and storage that may in turn lead to degradation/fragmentation, aggregation, and immunogenicity (9–11). However, while a number of studies have shown the effects of oxidative modifications such as methionine and cysteine oxidation on protein integrity, activity, and quality (12–15), little is known about the effect of oxidative carbonylation on therapeutic proteins. Previously, we had shown that the presence of trace amounts of transition metal Fe(II), H_2O_2, and ascorbic acid induced significant levels of carbonylation in proteins under moderate storage conditions (16). In order to gain further insight and assess analytical methodologies characterizing MCO-mediated oxidative modification, carbonylation, and protein degradation, we investigated bovine [Cu-Zn]-superoxide dismutase (bSOD1) treated with ascorbic acid/Cu(II) as a model system. bSOD1 was chosen because it is a biochemically stable metalloenzyme, requiring the Cu(II) and Zn(II) ions for catalytic activity and protein stability, respectively (17–19). The sites of protein oxidation and fragmentation by MCO have been proposed to be localized proximal to the metal binding sites (20,21). In addition, mutations in SOD1 have been identified to be responsible for ~10~20 % of the cases of the familial form of amyotrophic lateral sclerosis (fALS). Over 150 separate mutations scattered throughout the SOD1 molecules have been shown to induce ALS in an autosomal dominant fashion (22). While the mechanism of pathology induced by mutant SOD1 is yet to be clarified, the misfolding and aggregation of mutant SOD1 proteins has been proposed as the primary biochemical basis underlying the pathogenesis of fALS (23–25). Protein aggregation and inclusions are a common pathological hallmark of a number of neurodegenerative diseases such as Alzheimer's, Huntington's, and Parkinson's (26,27). Furthermore, oxidation of free cysteine or histidine residues in wild type SOD1 or the apoenzyme lacking both metal ions were shown to form oligomers, implicating involvement of wild type SOD1 oxidation as a possible factor for sporadic ALS that constitutes the majority of ALS cases (28–31).

Ascorbic acid, Cu(II), and oxygen from air are widely used to model MCO systems (1). Protein oxidation and fragmentation by MCO takes place in close proximity to the metal binding site as a consequence of extreme reactivity and the short life of the hydroxyl radical generated. Thus, MCO has been utilized to identify the metal binding sites of a number of proteins (32–35).

The comparative analyses of bSOD1 oxidized by ascorbic acid/Cu(II) and H_2O_2 described here, demonstrate a distinct pattern of protein fragmentation and effects on protein activity that were not previously recognized. Identification and characterization of the cleavage sites and the nature of oxidative modification unique to each reactive oxygen species (ROS) provide further insight into how proteins are modified by different oxidants, how sites of

modification are related to the protein structure, and how oxidative modifications impact protein integrity, quality, and activity.

Experimental procedures

Materials

Unless noted otherwise, all chemicals were obtained from Sigma-Aldrich (St. Louis, MO). Sigma supplied recombinant bovine SOD1 (Cat No. S9697) and catalase (Cat No. C9322). Sequencing grade trypsin and Asp-N protease were obtained from Promega (Madison, WI).

bSOD1 solution and activity

The lyophilyzed bSOD1 powder was dissolved in 20 mM Tris-HCl at pH 7.6. This was followed by buffer-exchange using a centrifuge filter, Amicon Ultra-0.5 MWCO 10K (Millipore, Billerica, MA) to remove trace amounts of free metal ions in the bSOD1 lyophilized powder. Using BSA as a standard, the protein concentration was determined by a modified Lowry assay (DC™ Protein Assay kit, Bio-Rad, Hercules, CA) and then adjusted to 1.6 mg/ml (50 μM) with the same buffer. It was then stored at −80°C. Activity was determined using an assay kit from Cayman Chemical (Ann Arbor, MI) according to the manufacturer's instructions.

bSOD1 treatment

The bSOD1 protein (final concentration 8–10 μM in 10 mM Tris-HCl, pH 7.6) was treated with the indicated concentration of additive in a 10–15 μl final volume for 30 minutes at 37°C. When the entire reaction mix was analyzed by SDS-PAGE, 4x LDS sample buffer (Life Technology, Grand Island, NY) was added directly and analyzed by SDS-polyacrylamide gel. Alternatively, the reaction was halted by addition of DTPA and/or catalase to achieve a final concentration of 100 μM and 5 ng/μl, respectively.

SDS-PAGE and quantitation of protein fragments

The bSOD1 reaction mix in LDS sample buffer with or without DTT (final 50 mM) were heated at 75°C for 10 min and analyzed on a 4–12% NuPAGE gel in Bis-Tris buffer using MES running buffer (Life Technologies, Grand Island, NY). After electrophoresis, the gel was fixed with 40% methanol/10% acetic acid, stained with SimplyBlue Safestain Coomassie Brilliant Blue (CBB) (Life Technologies), then destained with water. Protein in the bands was quantified utilizing the 700 nm channel of the Odyssey infrared imaging system (LI-COR, Lincoln, NE) and Image Studio software.

Carbonyl detection by western blot immunodetection

Western blot detection of the carbonyl moiety on bSOD1 was performed as described (36). In brief, the carbonyl in 0.4 μg of bSOD1 reaction mix were derivatized with 5 mM dinitrophenylhydrazine in 1 N HCl and 3% SDS for 10 minutes at room temperature, and then neutralized by the addition of 1 M Tris-base. After separation on a 4–12% NuPAGE gel, the dinitrophenyl-derivatized bSOD1 was transferred to PVDF membrane, hybridized with goat anti-dinitrophenyl (1:2,000 dilution) (Bethyl Laboratories, Montgomery, TX) and

donkey anti-goat secondary antibody IRDYe800CW conjugated (LI-COR, Cat No. 926-32214) and visualized with the Odyssey on the 800 channel.

Carbonyl quantitation by ELISA

The 0.02 μg dinitrophenyl-derivatized bSOD1 reaction mix was used for quantification by ELISA as recently described (16).

Reduction and alkylation and enzymatic digestion

Control (untreated) or Asc/Cu(II) treated bSOD was reduced with 5 mM DTT in 5 M guanidine-HCl at 37°C for 30 minutes, alkylated with 10 mM iodoacetamide (IAM) at 37°C for 30 minutes, and excess IAM was quenched by addition of 20 mM DTT. The reaction mix was desalted by binding the bSOD1 to a C18-tip column (Thermo-Pierce) followed by elution with 0.1% formic acid/50% acetonitrile according to the instructions of the manufacturer. For analysis of non-digested bSOD1, the eluate was adjusted to 4 pmol/ml and used for LC-MS analysis. For enzyme digestion, the bSOD1 eluate was dried *in vacuo*, dissolved in 60 μl of 25 mM ammonium bicarbonate buffer at a protein concentration of 10 pmol/μl. 30 μl of the solution was used for trypsin or Asp-N digestion at a substrate/enzyme ratio of 1:40 or 1:30, respectively. After 24 hours of digestion, formic acid was added to a final concentration of 0.1 % and the 5 μl of digests were analyzed.

Liquid chromatography-mass spectrometry (LC-MS) analysis

All LC-MS and tandem MS (MS/MS) analyses were conducted on an Agilent 1260 HPLC-Chip nano-electrospray-ionization 6520 Q-TOF MS system (LC-ESI-Q-TOF-MS). Solvent A was 0.1 % formic acid in water and Solvent B was 0.1 % formic acid in 95% acetonitrile. Mass correction was enabled during the run using internal reference ions with masses of 299.2945 and 1221.9906 Da. Intact protein mass measurement was performed using an Agilent 43 mm 300 A C8 chip with a 40 nL trap column (G4240-63001 SPQ105). The bSOD1 samples were diluted to 130 ng/μl (4 μM) in 0.1% formic acid, and at least 4 pmol (≥1 μl) was injected onto the trap column of the C8 chip at a flow rate of 2.5 μl/min in 100% Solvent A, then eluted at 0.5 μl/min with a linear gradient of 10–100% Solvent B for 18 minutes and held for an additional 4 minutes. The Q-TOF capillary voltage was 1,890 V and that of the fragmentor was 225 V. The nitrogen gas temperature was 350°C with a flow rate of 9 L/min. Data were analyzed with Agilent MassHunter and BioConfirm software (version B.05.00).

For peptide mapping by mass, the trypsin or Asp-N digested peptides were injected onto a 500 nL enrichment column in an Agilent Zorbax 150 mm 300 A C18 customizable chip at a flow rate of 2.5 μl/min in 100% Solvent A, then separated at 0.3 μl/min with a 55 minute gradient of 3–25% Solvent B in 35 minutes, 25–40% Solvent B in 10 minutes, 40–90% Solvent B in 5 minutes, and 90% Solvent B for 5 minutes. The drying gas flow rate was 9 L/min at 280°C. For data analysis, compounds were extracted using the “Find by Molecular Feature” function of MassHunter with the following settings: peak height ≥ 100 counts; isotopes groups with peak spacing tolerance of 0.0025 m/z and within 7.0 ppm using an isotope model for peptides; default charge states ≤ 8; and compound absolute height ≥ 5,000

counts. Peptides were mapped to the bSOD1 sequence with the “Define and Match Sequences” function of MassHunter with a mass tolerance of ± 5 ppm.

Peptide sequencing was first conducted with the auto-MS/MS acquisition method. Collision energy was ramped according to this formula for parent ions with 2+ charge: Collision Energy (eV) = 3.1 × m/z /100 + 1. For parent ions with >2+ charge, the formula was: Collision Energy (eV) = 3.6 × m/z /100 −4.8.

Certain selected parent ions of interest were also subjected to targeted MS/MS fragmentation using a range of fixed collision energy in 5 eV intervals, and one of the high quality MS/MS spectra was subjected to manual data analysis based on the expected ion masses calculated by GPMAW software (version 10.0, Lighthouse Data, Denmark). The associated collision energy is indicated in the figure legend.

Results

Ascorbic acid system cleaves bSOD1 at a site distinct from that of H_2O_2 system

To investigate the effects of MCO on the integrity and oxidative modification of bSOD1, bSOD1 was dissolved in Tris-HCl buffer at pH 7.6 and incubated with Asc, Fe(II), Cu(II), or H_2O_2 either alone or in combination for 30 minutes at 37°C. The treated bSOD1 samples were then analyzed by SDS-PAGE under reducing and non-reducing conditions (Fig. 1). As shown in lanes 5,11, and 12, incubation of bSOD1 with H_2O_2 with or without transition metals Cu(II) or Fe(II) generated 9.5 and 6.5 kDa cleavage products (indicated by solid arrows), a fragmentation pattern demonstrated previously for human [Cu-Zn]-SOD (37). In these samples, dimers were observed under non-reducing conditions (Fig 1 lower panel) indicating the formation of an interchain disulfide bond. In contrast, bSOD1 samples treated with Asc in combination with Cu(II) and/or H_2O_2 showed a distinct pattern of fragmentation with 12.5 and 3.2 kDa cleavage products indicated by open arrows (lanes 6, 8, and 9). Furthermore, presence of Asc counteracted the H_2O_2-specific fragmentation and dimerization patterns (lane 8). Notably, the Asc-specific fragmentation was inhibited by the presence of Fe (II) but enhanced by the presence of Cu(II) (lane 8 vs. lane 9 or 10) indicating very distinct roles played by Cu(II) and Fe(II), two transition metals that have been widely used in MCO of proteins (1, 38). Asc is a scavenger of hydroxyl radical and because of that activity, Asc has been used to limit H_2O_2 mediated non-specific oxidation of bSOD1 (38). Because the observations with Asc presented in Figure 1 were different from a previous report concerning Asc and H_2O_2 mediated SOD1 fragmentation, we further investigated Asc-mediated fragmentation and oxidation of bSOD1 to understand the underlying mechanism.

Comparison of bSOD1 fragmentation mediated by Asc vs. H_2O_2

First, we investigated the essential component required for Asc-mediated fragmentation of bSOD1 (Fig. 2). The results in lanes 1–3 in Fig. 2A demonstrates that Cu(II) is essential for Asc-mediated fragmentation Thus, the Asc/H_2O_2/Cu(II)-mediated fragmentation was completely blocked by the addition of metal chelator DTPA and was restored by the addition of Cu(II) whose concentration exceeded that of DTPA. In contrast, the H_2O_2-mediated

fragmentation appeared to be independent of added metal. An excess amount of DTPA over Cu(II) or Fe(II) (Fig. 2A lanes 8 and 9), or addition of a higher concentration of transition metal to DTPA containing sample had little effect on the fragmentation mediated by 1 mM H_2O_2. These observations are in line with that of H_2O_2 mediated fragmentation utilizing catalytic site-bound copper ion that is tightly coordinated by histidine residues and is not stripped by DTPA. To further investigate the components that are essential for bSOD1 fragmentation, we titrated different concentrations of Asc, Cu(II), and H_2O_2 either alone or in a combination. As shown in Fig. 2B, lane 4, a high concentration (100 mM) of Asc alone generated a low level of fragmentation. In reactions where 5 mM Asc was used, maximum cleavage was obtained with 30 μM Cu(II) (lane 6). Addition of H_2O_2 to 5 mM Asc generated a moderate level of fragmentation in a concentration dependent manner (lanes 8–11). Little effect on fragmentation was observed by increasing the concentration of Asc or Cu(II) in the reaction mixtures of 5 mM Asc/1 mM H_2O_2/10 μM Cu(II) (Fig 2B, lane 12 vs. lanes 13–16). It should be noted that Asc plus H_2O_2 treatment heavily favored an Asc-specific cleavage pattern as shown in previous figures. Thus, these results indicate that Asc and Cu(II) are sufficient to achieve cleavage, but H_2O_2 also facilitates fragmentation in reactions lacking added Cu(II) ion.

Fe(II) and Cr(II) blocks the Asc/Cu(II)-mediated fragmentation

Seemingly contradictory to the role of Fe ion in MCO, our results indicated that Fe ion blocks the Asc/Cu(II)-mediated bSOD1 fragmentation. To understand the chemical basis for this inhibition and whether the inhibition is common to other transition metals, we tested the effects of several transition metals on Asc/Cu(II)-mediated fragmentation (Fig. 3A and quantified in 3B). Significant inhibitory effects were observed only with Fe(II) and high concentrations of Cr(II) [1 mM: 30 fold excess concentration of Cu(II) ion] while other transition metals tested showed no significant inhibitory or stimulatory activity. Fig. 3C demonstrated that the inhibition of fragmentation by Fe(II) is concentration dependent and ~50% inhibition was achieved in the presence of 30 μM Fe(II). Collectively, these results confirm that Fe(II), and to a lesser degree Cr(II), potentially compete with copper ion at the new putative metal binding site of bSOD1 and block bSOD1 fragmentation that is mediated specifically by copper ion as implicated by the initial observation shown in Fig. 1.

The Asc/Cu(II)-mediated fragmentation is resistant to catalase

To delineate further the Asc/Cu(II)-mediated bSOD1 fragmentation from H_2O_2-mediated fragmentation, we tested the effect of catalase on the fragmentation of bSOD1 (Fig. 3D). We show that co-incubation with catalase does not block Asc/Cu(II)-dependent fragmentation; an excess amount of catalase (1 μg=2.8 units) was required to observe significant inhibition in fragmentation of 8 pmol bSOD1. Thus, the Asc/Cu(II)-mediated bSOD1 fragmentation is not dependent on hydrogen peroxide being accessible to catalase.

Oxidation/Carbonylation of bSOD1

The side chains of arginine, lysine, threonine, and proline residues are prone to MCO and as a consequence, carbonyl moieties (aldehyde and ketones) are incorporated into the protein (1,3). Carbonylation under excessive ROS may be associated with protein fragmentation (2). We investigated Asc/Cu(II)-mediated oxidation/carbonylation and compared it to the H_2O_2-

mediated oxidation/carbonylation (Fig. 4, A–D). bSOD1 was treated under various conditions and the carbonyl levels were determined by western blot immunodetection and ELISA (Fig. 4A and 4D). As shown in lanes 2, 4 and 5, either 5 mM Asc alone, 30 μM Cu(II) or 30 μM Fe(II) alone did not induce significant carbonylation. In contrast, exposure to 1 mM H_2O_2 (lane 3) induced 10–12 nmol carbonyl/mg bSOD1 (~0.3 mol carbonyl/mol bSOD1). Carbonylation by H_2O_2 was not dependent on exogenous metal as addition of Cu(II), Fe(II), or metal chelator DTPA to the reaction with H_2O_2 did not significantly impact carbonylation (lane 3 vs. lanes 11,12, and 14). Although 5 mM Asc alone did not induce carbonylation, addition of 30 μM Cu(II) (lane 7) induced bSOD1 carbonylation at a level slightly higher than H_2O_2 alone. Maximum oxidation was observed in the reaction treated with a combination of Asc, Cu(II), and H_2O_2 (lane 9). In contrast to Cu(II), addition of Asc to H_2O_2/Fe(II) completely blocked the H_2O_2-dependent oxidation (lanes 3 and 11 vs. lane 10). Furthermore, comparison of reactions in lane 6 and lane 10 also confirmed Fe(II) interference with Asc/H_2O_2-mediated oxidation. Finally, the quantitation of carbonyl in fragments (shown by the values under the enhanced image in Fig. 4B) and abundance of fragment relative to the intact 15.5 KDa band in the CBB stained gel image (Fig. 4C) indicated that the majority of carbonyl moieties are localized to the non-cleaved full length bSOD1.

Enzyme activity of bSOD1 treated with Asc/Cu(II) or H_2O_2

The oxidative modification of SOD1 by H_2O_2 was shown to be associated with a loss of enzymatic activity that precedes fragmentation/degradation and takes place in a two step reaction: cleavage at Pro62-His63 that does not require exogenous transition metal, and a second, transition metal-dependent non-specific random fragmentation (37,39,40). To further understand the chemistry underlying Asc/Cu(II)-mediated fragmentation and oxidation, we investigated the enzymatic activity of Asc/Cu(II) treated bSOD1 and compared it to H_2O_2 treated bSOD1 (Fig. 4E). The results showed that in contrast to H_2O_2 mediated oxidation, the Asc/Cu(II) treatment did not inactivate bSOD1 at 30 minutes establishing that the 12.5 kDa fragment retains its enzymatic activity. Furthermore, the presence of Asc abrogates H_2O_2-induced inactivation as shown for bSOD1 samples treated with Asc/Cu(II)+H_2O_2 or Asc+H_2O_2. The observed abrogation with Asc is in agreement with previous reports that Asc decomposes peroxide (41).

Identifying the cleavage site(s) on Asc/Cu(II)-treated bSOD1 by LC-MS at intact protein mass level

The distinct cleavage and carbonylation of bSOD1 with Asc/Cu(II) compared to the previously reported H_2O_2 prompted us to further investigate the biochemical mechanism and site(s) of fragmentation. To this end, first, untreated bSOD1 and AsA/Cu(II)-treated bSOD1 were analyzed by LC-ESI-Q-TOF-MS at intact protein mass level. Fig. 5(A–C) shows the deconvoluted mass spectra for control (untreated) and Asc/Cu(II)-treated bSOD1. The major peak at 15,722.56 Da of control bSOD1 matched well to the theoretical average molecular mass 15,722.51Da for the reduced and alkylated full-length bSOD1 (Ala1-Lys151). The spectrum of Asc/Cu(II)-treated bSOD1 showed mass peaks at 15,722.23, 15,737.64, 15,753.36, 15,768.64 Da and minor peaks with higher molecular mass implicating modification of bSOD1 by Asc/Cu(II) (Fig 5B). Multiple peaks were also observed around

12.5 kDa, e.g. 12,584.76, 12,599.35, 12,611,37, 12,626.57, 12,640.79 and 12,657.21 Da (Fig 5C). These peaks likely correspond to the Asc/Cu(II) cleavage products shown in SDS-PAGE images in Fig. 1–4. Among them, the 12,584.76 mass matched well to the theoretical mass of 12584.90 Da for bSOD1 C-terminal fragment Ser32-Lys151 while 12,640.79 is 1 Da lower than 12,641.96 Da, the theoretical mass of fragment Gly31-Lys151. These data indicate the cleavage by Asc/Cu(II) had likely taken place at Gly31. The other major peak with mass 12,611.37 Da was assigned to Ser32-Lys151 fragment with an N-terminus isocyanate modification based on identification of an Asp-N peptide Ser32-Gly39 with this modification (see Fig. 6B). Other observed masses did not match with any theoretical masses of potential bSOD1 fragments indicating additional oxidative modification of these fragments.

LC-Q-TOF-MS/MS analysis of peptide pinpoints the cleavage site at Gly31

In order to precisely locate the cleavages site(s) and elucidate a biochemical basis of reaction that leads to bSOD1 cleavage, it was essential to identify and characterize peptides that span the cleavages site(s). To this end, first we established the LC-MS conditions to allow 100% sequence coverage based on peptide mass mapping of the tryptic and Asp-N digest of control and Asc/Cu(II)-treated bSOD1 (Supplementary Fig. S1, Table S1, and Table S2). Then we focused on identifying peptides that were unique to Asc/Cu(II)-treated bSOD1. If bSOD1 is cleaved at Gly31, as suggested by LC-MS analysis of non-enzyme digested Asc/Cu(II)-treated bSOD1 (Fig. 5D), new tryptic and Asp-N peptides should be generated from the indicated T4 and D3 peptides that span the cleavage site (Fig. 5D and Supplementary Fig. S1A and S1B). According to the proposed protein oxidative cleavage reaction (2,42), following the abstraction of an α-hydrogen at Gly31, a carbon-centered free radical derivative of bSOD1 is generated. carbon-centered radical thus formed is readily converted to alkoxyl radical leading to the cleavage of bSOD1 backbone at either side of Gly31 through the diamide or α-amidation pathways. The diamide pathway then generates an N-terminal fragment Ala1-Thr30 and C-terminal fragment Ser32-Lys151, whereas the cleavage through the α-amidation pathway generates Ala1-Thr30 and Gly31-Lys151 with Thr30 and Gly31 residues being amidated or α-ketoacylated, respectively (Table 1). Based on these two hypothetical pathways, the possible tryptic or Asp-N peptides and their theoretical molecular masses were calculated (Table 1, columns 2–4). Also included in Table 1 are peptides with N-terminal isocyanate modification at Ser32, the intermediate product of the diamide pathway.

Next, we screened all compounds detected by LC-Q-TOF-MS peptide analysis and as shown in Table 1 column 5, we identified all peptides with molecular mass closely matched to those of predicted peptides. The primary structure of the peptides were then determined utilizing targeted LC-MS/MS analysis of trypsin and Asp-N digests of Asc/Cu(II)-treated bSOD1 (Fig. 6 and 7). Shown in Fig. 6 are MS/MS spectra for Asp-N peptides with masses of 776.39 Da and 802.38 Da corresponding to unmodified and isocyanate modified Ser32-Gly39, respectively. The 776.39 Da peptide was confirmed as Ser32-Gly39 (Fig. 6A). For the 802.28 Da peptide, the b ions were identified on the assumption that the N-terminus Ser32 was modified to isocyanate giving a mass shift of +25.98 Da (+C+O-2H), while y ions were identified without any changes. Identification of the [b3] – [b7] ions and y2 – y6 ions

confirmed that the +25.98 Da mass shift is derived from either the N-terminal Ser32 or Ile33. This result strongly suggests that the 26 Da mass shift corresponds to an isocyanate modification at the N-terminus amino acid of the C-terminal fragment generated through the diamide pathway.

The MS/MS spectra of Asp-N peptides with mass 631.35 and 832.38 Da are shown in Fig. 7. The mass of these peptides matched those generated through the μ-amidation pathway. The y ions of mass 631.35 Da peptide were identified assuming amide modification at the C-terminal Thr30 that gave a −0.98 Da shift (+N+2H−OH) for y ions. The b ions were assigned without any changes (Fig. 7A). Thus, identification of b2 – b5 and [y1] – [y3] ions confirmed the sequence of the peptide and assigned the 0.98 Da mass shift to modification at Thr30. Similarly, as shown in Fig. 7B, the b ions of 832.38 Da peptide (Gly31–Gly39) were identified assuming the modification at Gly31 to be an α-ketoacyl derivative produced via the α-amidation pathway. This modification would confer a −1.03 Da mass shift (+O−NH3) from the non-modified Gly31–Gly39 peptide (theoretical mass of 833.44 Da). The assignment of [b4] – [b8] and y2 – y6 ions identified the modification on one of three N terminal amino acids residues.

The precise cleavage site and its mode of cleavage reaction were also confirmed by analysis of tryptic peptides listed in Table 1 column 5 (Supplementary Fig. S2–S5). In conclusion, utilizing LC-Q-TOF-MS/MS analysis, we localized the cleavage site mediated by Asc/Cu(II) to Gly31-Ser32 and Thr30-Gly31 of the bSOD1 protein molecule. Identification and characterization of Asp-N and tryptic peptides implicated a carbon centered radical generation at α-carbon of Gly31 that then produced an alkoxyl radical followed by cleavage of the protein backbone on either side of Gly31 through the diamide or α-amidation pathway.

Asc/Cu(II) specific novel modifications in bSOD1 as a consequence of Cu binding to new metal binding site

The deconvoluted spectra of Asc/Cu-treated SOD1 showed multiple peaks that significantly differ from those seen in the untreated control SOD1 protein indicating oxidative modification. To identify the modification, both tryptic and Asp-N digests of bSOD1 samples were subjected to data-dependent as well as targeted MS/MS analysis. Utilizing the same approach as used for identifying Asp-N and tryptic fragments generated through cleavages in Asc/Cu-treated bSOD1, we identified two fragments that were unique to digest of Asc/Cu-treated bSOD1. His19 oxidation to oxo-histidine was identified from mass 1,470.71 Da tryptic peptide(Fig. 8A) and Lys3 oxidation to delta-hydroxy-allysine was identified from the analysis of mass 1,060.56 Asp-N peptide (Fig. 8B). Notably, these modifications are unique to only Asc/Cu-treated SOD1 as they were not detected by H_2O_2 treated protein.

Discussion

Mechanism of bSOD1 fragmentation by Asc and copper ion

We investigated MCO utilizing an Asc/Cu(II) system focusing on oxidation/carbonylation and cleavage of the bSOD1 molecule. Comparative analysis with bSOD1 treated by H_2O_2 demonstrated the unique activity of Asc that exerts distinct biochemical effects on bSOD1 by interacting with added copper ion. This may be explained by considering firstly, possible binding of copper or iron ion to the bSOD1 surface at site(s) distinct from the catalytic copper binding site, and secondly, opposing activities of Asc by acting as an antioxidant that scavenges free radicals and at the same time generates reactive oxygen species through a Fenton-like reaction (43,44). Based on our data, we propose the following biochemical mechanism (summarized in Fig. 9). First, bSOD1 molecule with Cu(I) ion bound to a non-catalytic site-[bSOD1/Cu^{2+}−Cu(I)] is formed. Under one possible scheme, Cu(II) is reduced to Cu(I) by ascorbate following binding to the bSOD1 (reaction1a and 1b) or alternatively reduced in aqueous phase prior to the binding(reaction 1c). In a second reaction, Cu(I) is either oxidized directly by molecular oxygen or H_2O_2 generated from Cu(II)-catalyzed reduction of molecular oxygen(O_2) and ascorbate (AH-). The reactive oxygen species generated must be localized in close proximity to the copper-binding site as is known for caged free radicals because the cleavage is catalase resistant. Consistent with this hypothesis, radical scavengers such at DMSO and mannitol did not block the reaction (data not shown). In a final step, the hydroxyl radical abstract the nearby α-hydrogen atom from the polypeptide chain forming a carbon-centered radical. The carbon-centered radical undergoes rapid reaction with oxygen to form a peroxyl radical intermediate which is radially converted to protein peroxide in presence of H^+ and Fe^{2+} or $HO_2^{\bullet}$. Protein peroxide thus formed undergoes dismutation reaction to form alkoxyl radical that leads to protein backbone cleavage through the diamide or α-amidation pathways (2,42). This proposed mechanism may further explain the inhibitory effect of other transition metals. Thus, the inhibition by Fe(II) may be attributed to the competitive binding of iron to the copper binding site, Fe(II) is a significantly poorer electron donor in the cleavage of thyrotropin-releasing-hormone precursor peptide as compared to Cu(II) (45). The Cu(II)-ascorbate system appears more effective at inactivating enzymes than Fe(II)-ascorbate but there are no reports to demonstrate that Fe(II) completely protects proteins against Cu(II)-ascorbate mediate fragmentation or inactivation (33,46). Although reproducible, currently we do not have an explanation for why only Fe(II) is effective to protect bSOD1 against Cu(II)-ascorbate mediated fragmentation (Figure 3B). It is possible that Fe(II) binds in a separate binding site close proximity to the Cu(II) binding site. The hydroxyl radicals may be reduced via Fe(II) before attacking the Gly31 because the rate constant for the hydroxyl radical with Gly is significantly smaller compared to the reaction of hydroxyl radical with Fe(II). High levels of Asc-specific fragmentation and carbonylation are also generated in a reaction where Asc and H_2O_2 are present but not Cu(II) (Fig 1, 2, and 4). Under these conditions, the reaction could utilize copper ion released from the catalytic site of bSOD1 holoenzyme. The initial reaction with H_2O_2 mediates oxidation and fragmentation of bSOD1 that leads to inactivation, denaturation of intact bSOD1 and release of catalytic copper ion (37,47,48). Once the copper ion is available, the overall reaction may shift towards the Asc/Cu(II) specific reaction. Supporting this assumption, examination of CBB

stained Asc/H_2O_2 showed a 9.5 kDa fragment specific to H_2O_2-mediated cleavage (for example, lane 10 in Fig. 2B).

It is also possible that the proximal oxidant is Cu(II)OH or Cu(III), which could be produced by reduction of Cu(II) by ascorbate to Cu(I), which in turn could react with peroxide and yield Cu(II)OH or Cu(III).

Asc/Cu(II)-specific fragmentation

Hydrogen peroxide mediates bSOD1 oxidation and fragmentation at copper-coordinating His residues (His44, His46 and His116) and Pro60, Val116 and Val11 [or Pro62 and His63 in human SOD1] and cleavage at Pro61-His62 (20,21,37). The modification and cleavage at the specific sites indicate that the oxidative modification and cleavage by H_2O_2 are tertiary structure dependent. Given that H_2O_2 is a product of the dismutase reaction, there exists a binding site for H_2O_2 at the active site. Fragmentation is mediated by hydroxyl radicals generated from a Fenton-type reaction with a catalytic site-bound Cu (II) and H_2O_2. Importantly, our results showed Asc suppresses the H_2O_2 specific fragmentation pattern and oxidation/carbonylation (as shown in lane 3 vs. lanes 6 and 9 in Fig. 4A–C). This inhibition was also observed in the presence of Fe(II) ion, where Asc dependent fragmentation and oxidation were blocked (lane 10 Fig. 4A–C).

Identification of the cleavage site and determination of the end structure of fragments

The data acquired by LC-MS and LC-MS/MS provided evidence for exact location of the cleavage and the underlying mechanism. The detection and sequence determination of Asp-N peptides indicated that the cleavage of bSOD1 took place at Gly31-Ser32 and Thr30-Gly31. Examination of the crystal structure of bSOD1 for potential copper binding site(s) including His, Asn, Gln, Glu, and Cys residues showed that the imidazole ring of His19 is located within 5 Angstrom of the α-carbon of Gly31 (Fig. 10), thus providing structural basis that the copper ion, most likely bound to bSOD1 protein surface through coordination involving His19 and Gly31(49), and H_2O_2 generated at the binding site (Reaction 2) catalyzes the specific cleavage reaction at the Thr30-Gly31 or Gly31-Ser32 bond. Investigations by LC-MS/MS indicated oxidative modification of His19 to oxo-His and Lys3 to allysine in Asc/Cu(II) treated bSOD1 but not control untreated bSOD1. The imidazole ring of His19 and the amino group of Lys3 are both exposed to solvent and located within 10 angstroms. These findings further suggest that His19 is involved in binding of a third metal in bSOD1 which in turn mediates its own oxidation or Lys3 modification due to site specific generation of hydroxyl radical as described in Fig 9. Fig. 10A shows the putative copper coordinating amino acid residues relative to catalytic copper ion in the bSOD1 homodimer and Fig. 10B demonstrates the close proximity of His19, Thr30, and Gly31. In line with the bSOD1 findings, preliminary investigations on Asc/Cu(II) mediated fragmentation of human [Cu-Zn]-SOD1 indicated the Asc/Cu(II) system cleaves human SOD1 at specific site(s) distinct from those mediated by H_2O_2. Therefore, the finding reported here is likely applicable to human [Cu-Zn]-SOD1. Intracellular copper is tightly controlled by copper binding protein and free copper concentration is extremely low (50), thus it is unlikely that Cu(II) and Asc dependent cleavage reported here is taking place under physiological conditions [for a discussion on possible roles of ascorbic acid *in vivo* see comments by

Halliwell (43) and Carr and Frei (51)]. It has been proposed that misfolding and subsequent aggregation of wild type [Cu-Zn]-SOD1 play a role in etiology of sporadic ALS (52). If misfolding/aggregation can be triggered by oxidative modification of wild type SOD1 (53,54), the effective antioxidant activity of Asc or other agents against excessive ROS could be a potentially effective therapeutic target for intervention of sporadic ALS initiation or progression.

Supplementary Material

Refer to Web version on PubMed Central for supplementary material.

Acknowledgments

This research was supported by the FDA CDER Critical Path Initiative. RLL was supported by the Intramural Research Program of the National Heart, Lung, and Blood Institute. We would like to thank Dr. Dmitry Kryndushkin and Elliot Rosen (FDA) for critical reading of the manuscript.

Abbreviations

bSOD1	bovine [Cu-Zn]-superoxide dismutase
MCO	metal catalyzed oxidation
ALS	amyotrophic lateral sclerosis
ROS	reactive oxygen species
Asc	sodium ascorbate
LC-ESI-Q-TOF-MS	liquid chromatography-electrospray ionization-quadrupole-time of flight-mass spectrometry
DTPA	diethylene-triamine-penta-acetic acid
CBB	Coomassie Brilliant Blue

References

1. Stadtman ER. Metal ion-catalyzed oxidation of proteins: biochemical mechanism and biological consequences. Free radical biology & medicine. 1990; 9:315–325. [PubMed: 2283087]
2. Berlett BS, Stadtman ER. Protein oxidation in aging, disease, and oxidative stress. J Biol Chem. 1997; 272:20313–20316. [PubMed: 9252331]
3. Amici A, Levine RL, Tsai L, Stadtman ER. Conversion of amino acid residues in proteins and amino acid homopolymers to carbonyl derivatives by metal-catalyzed oxidation reactions. J Biol Chem. 1989; 264:3341–3346. [PubMed: 2563380]
4. Levine RL, Williams JA, Stadtman ER, Shacter E. Carbonyl assays for determination of oxidatively modified proteins. Methods in enzymology. 1994; 233:346–357. [PubMed: 8015469]
5. Nystrom T. Role of oxidative carbonylation in protein quality control and senescence. The EMBO journal. 2005; 24:1311–1317. [PubMed: 15775985]
6. Dalle-Donne I, Giustarini D, Colombo R, Rossi R, Milzani A. Protein carbonylation in human diseases. Trends in molecular medicine. 2003; 9:169–176. [PubMed: 12727143]

7. Dalle-Donne I, Rossi R, Giustarini D, Milzani A, Colombo R. Protein carbonyl groups as biomarkers of oxidative stress. Clinica chimica acta; international journal of clinical chemistry. 2003; 329:23–38.
8. Levine RL, Garland D, Oliver CN, Amici A, Climent I, Lenz AG, Ahn BW, Shaltiel S, Stadtman ER. Determination of carbonyl content in oxidatively modified proteins. Methods in enzymology. 1990; 186:464–478. [PubMed: 1978225]
9. Torosantucci R, Schoneich C, Jiskoot W. Oxidation of therapeutic proteins and peptides: structural and biological consequences. Pharmaceutical research. 2014; 31:541–553. [PubMed: 24065593]
10. Shacter E. Quantification and significance of protein oxidation in biological samples. Drug metabolism reviews. 2000; 32:307–326. [PubMed: 11139131]
11. Jenkins N, Murphy L, Tyther R. Post-translational modifications of recombinant proteins: significance for biopharmaceuticals. Molecular biotechnology. 2008; 39:113–118. [PubMed: 18327554]
12. Bertolotti-Ciarlet A, Wang W, Lownes R, Pristatsky P, Fang Y, McKelvey T, Li Y, Li Y, Drummond J, Prueksaritanont T, Vlasak J. Impact of methionine oxidation on the binding of human IgG1 to Fc Rn and Fc gamma receptors. Molecular immunology. 2009; 46:1878–1882. [PubMed: 19269032]
13. Gaza-Bulseco G, Faldu S, Hurkmans K, Chumsae C, Liu H. Effect of methionine oxidation of a recombinant monoclonal antibody on the binding affinity to protein A and protein G. Journal of chromatography B, Analytical technologies in the biomedical and life sciences. 2008; 870:55–62. [PubMed: 18567545]
14. Lu HS, Fausset PR, Narhi LO, Horan T, Shinagawa K, Shimamoto G, Boone TC. Chemical modification and site-directed mutagenesis of methionine residues in recombinant human granulocyte colony-stimulating factor: effect on stability and biological activity. Archives of biochemistry and biophysics. 1999; 362:1–11. [PubMed: 9917323]
15. Yan B, Yates Z, Balland A, Kleemann GR. Human IgG1 hinge fragmentation as the result of H2O2-mediated radical cleavage. J Biol Chem. 2009; 284:35390–35402. [PubMed: 19850927]
16. Uehara H, Rao VA. Metal-mediated protein oxidation: applications of a modified ELISA-based carbonyl detection assay for complex proteins. Pharmaceutical research. 2015; 32:691–701. [PubMed: 25182973]
17. Rakhit R, Chakrabartty A. Structure, folding, and misfolding of Cu,Zn superoxide dismutase in amyotrophic lateral sclerosis. Biochimica et biophysica acta. 2006; 1762:1025–1037. [PubMed: 16814528]
18. Perry JJP, Shin DS, Getzoff ED, Tainer JA. The structural biochemistry of the superoxide dismutases. Biochimica et biophysica acta. 2010; 1804:245–262. [PubMed: 19914407]
19. Arnesano F, Banci L, Bertini I, Martinelli M, Furukawa Y, O'Halloran TV. The unusually stable quaternary structure of human Cu,Zn-superoxide dismutase 1 is controlled by both metal occupancy and disulfide status. J Biol Chem. 2004; 279:47998–48003. [PubMed: 15326189]
20. Kurahashi T, Miyazaki A, Suwan S, Isobe M. Extensive investigations on oxidized amino acid residues in H(2)O(2)-treated Cu,Zn-SOd protein with LC-ESI-Q-TOF-MS, MS/MS for the determination of the copper-binding site. Journal of the American Chemical Society. 2001; 123:9268–9278. [PubMed: 11562208]
21. Uchida K, Kawakishi S. Identification of oxidized histidine generated at the active site of Cu,Zn-superoxide dismutase exposed to H2O2. Selective generation of 2-oxo-histidine at the histidine 118. J Biol Chem. 1994; 269:2405–2410. [PubMed: 8300566]
22. Abel O, Powell JF, Andersen PM, Al-Chalabi A. ALSoD: A user-friendly online bioinformatics tool for amyotrophic lateral sclerosis genetics. Human mutation. 2012; 33:1345–1351. [PubMed: 22753137]
23. Bruijn LI, Houseweart MK, Kato S, Anderson KL, Anderson SD, Ohama E, Reaume AG, Scott RW, Cleveland DW. Aggregation and motor neuron toxicity of an ALS-linked SOD1 mutant independent from wild-type SOD1. Science (New York, N Y). 1998; 281:1851–1854.
24. Rakhit R, Robertson J, Vande Velde C, Horne P, Ruth DM, Griffin J, Cleveland DW, Cashman NR, Chakrabartty A. An immunological epitope selective for pathological monomer-misfolded SOD1 in ALS. Nature medicine. 2007; 13:754–759.

25. Wang J, Xu G, Borchelt DR. High molecular weight complexes of mutant superoxide dismutase 1: age-dependent and tissue-specific accumulation. Neurobiology of disease. 2002; 9:139–148. [PubMed: 11895367]
26. Taylor JP, Hardy J, Fischbeck KH. Toxic proteins in neurodegenerative disease. Science (New York, N Y). 2002; 296:1991–1995.
27. Caughey B, Lansbury PT. Protofibrils, pores, fibrils, and neurodegeneration: separating the responsible protein aggregates from the innocent bystanders. Annual review of neuroscience. 2003; 26:267–298.
28. Bosco DA, Morfini G, Karabacak NM, Song Y, Gros-Louis F, Pasinelli P, Goolsby H, Fontaine BA, Lemay N, McKenna-Yasek D, Frosch MP, Agar JN, Julien J-P, Brady ST, Brown RH Jr. Wild-type and mutant SOD1 share an aberrant conformation and a common pathogenic pathway in ALS. Nature neuroscience. 2010; 13:1396–1403. [PubMed: 20953194]
29. Furukawa Y. Pathological roles of wild-type cu, zn-superoxide dismutase in amyotrophic lateral sclerosis. Neurology research international. 2012; 2012:323261. [PubMed: 22830015]
30. Furukawa Y, O'Halloran TV. Amyotrophic lateral sclerosis mutations have the greatest destabilizing effect on the apo- and reduced form of SOD1, leading to unfolding and oxidative aggregation. J Biol Chem. 2005; 280:17266–17274. [PubMed: 15691826]
31. Guareschi S, Cova E, Cereda C, Ceroni M, Donetti E, Bosco DA, Trotti D, Pasinelli P. An over-oxidized form of superoxide dismutase found in sporadic amyotrophic lateral sclerosis with bulbar onset shares a toxic mechanism with mutant SOD1. Proc Natl Acad Sci U S A. 2012; 109:5074–5079. [PubMed: 22416121]
32. Hlavaty JJ, Nowak T. Affinity cleavage at the metal-binding site of phosphoenolpyruvate carboxykinase. Biochemistry. 1997; 36:15514–15525. [PubMed: 9398280]
33. Chou WY, Tsai WP, Lin CC, Chang GG. Selective oxidative modification and affinity cleavage of pigeon liver malic enzyme by the Cu(2+)-ascorbate system. J Biol Chem. 1995; 270:25935–25941. [PubMed: 7592782]
34. Soundar S, Colman RF. Identification of metal-isocitrate binding site of pig heart NADP-specific isocitrate dehydrogenase by affinity cleavage of the enzyme by Fe(2+)-isocitrate. J Biol Chem. 1993; 268:5264–5271. [PubMed: 8444900]
35. Hovorka SW, Williams TD, Schoneich C. Characterization of the metal-binding site of bovine growth hormone through site-specific metal-catalyzed oxidation and high-performance liquid chromatography-tandem mass spectrometry. Analytical biochemistry. 2002; 300:206–211. [PubMed: 11779112]
36. Shacter E, Williams JA, Lim M, Levine RL. Differential susceptibility of plasma proteins to oxidative modification: examination by western blot immunoassay. Free radical biology & medicine. 1994; 17:429–437. [PubMed: 7835749]
37. Ookawara T, Kawamura N, Kitagawa Y, Taniguchi N. Site-specific and random fragmentation of Cu,Zn-superoxide dismutase by glycation reaction. Implication of reactive oxygen species. J Biol Chem. 1992; 267:18505–18510. [PubMed: 1326527]
38. Bridgewater JD, Vachet RW. Metal-catalyzed oxidation reactions and mass spectrometry: the roles of ascorbate and different oxidizing agents in determining Cu-protein-binding sites. Analytical biochemistry. 2005; 341:122–130. [PubMed: 15866536]
39. Jewett SL, Rocklin AM, Ghanevati M, Abel JM, Marach JA. A new look at a time-worn system: oxidation of CuZn-SOD by H2O2. Free radical biology & medicine. 1999; 26:905–918. [PubMed: 10232834]
40. Salo DC, Pacifici RE, Lin SW, Giulivi C, Davies KJ. Superoxide dismutase undergoes proteolysis and fragmentation following oxidative modification and inactivation. J Biol Chem. 1990; 265:11919–11927. [PubMed: 2195028]
41. Deutsch JC. Ascorbic acid oxidation by hydrogen peroxide. Analytical biochemistry. 1998; 255:1–7. [PubMed: 9448835]
42. Garrison WM, Kland-English M, Sokol HA, Jayko ME. Radiolytic degradation of the peptide main chain in dilute aqueous solution containing oxygen. The Journal of physical chemistry. 1970; 74:4506–4509. [PubMed: 5494901]

43. Halliwell B. Vitamin C: antioxidant or pro-oxidant in vivo? Free radical research. 1996; 25:439–454. [PubMed: 8902542]
44. Stadtman ER. Ascorbic acid and oxidative inactivation of proteins. The American journal of clinical nutrition. 1991; 54:1125S–1128S. [PubMed: 1962558]
45. Bateman RC Jr, Youngblood WW, Busby WH Jr, Kizer JS. Nonenzymatic peptide alpha-amidation. Implications for a novel enzyme mechanism. J Biol Chem. 1985; 260:9088–9091. [PubMed: 3926762]
46. Tang SS, Lin CC, Chang GG. Metal-catalyzed oxidation and cleavage of octopus glutathione transferase by the Cu(II)-ascorbate system. Free radical biology & medicine. 1996; 21:955–964. [PubMed: 8937881]
47. Sato K, Akaike T, Kohno M, Ando M, Maeda H. Hydroxyl radical production by H2O2 plus Cu,Zn-superoxide dismutase reflects the activity of free copper released from the oxidatively damaged enzyme. J Biol Chem. 1992; 267:25371–25377. [PubMed: 1334093]
48. Jewett SL, Cushing S, Gillespie F, Smith D, Sparks S. Reaction of bovine-liver copper-zinc superoxide dismutase with hydrogen peroxide. Evidence for reaction with H2O2 and HO2- leading to loss of copper. European journal of biochemistry/FEBS. 1989; 180:569–575. [PubMed: 2714271]
49. Carrera F, Marcos ES, Merkling PJ, Chaboy J, Munoz-Paez A. Nature of metal binding sites in Cu(II) complexes with histidine and related N-coordinating ligands, as studied by EXAFS. Inorg Chem. 2004; 43:6674–6683. [PubMed: 15476367]
50. Rae TD, Schmidt PJ, Pufahl RA, Culotta VC, O'Halloran TV. Undetectable intracellular free copper: the requirement of a copper chaperone for superoxide dismutase. Science (New York, N Y). 1999; 284:805–808.
51. Carr A, Frei B. Does vitamin C act as a pro-oxidant under physiological conditions? FASEB journal: official publication of the Federation of American Societies for Experimental Biology. 1999; 13:1007–1024. [PubMed: 10336883]
52. Deng H-X, Shi Y, Furukawa Y, Zhai H, Fu R, Liu E, Gorrie GH, Khan MS, Hung W-Y, Bigio EH, Lukas T, Dal Canto MC, O'Halloran TV, Siddique T. Conversion to the amyotrophic lateral sclerosis phenotype is associated with intermolecular linked insoluble aggregates of SOD1 in mitochondria. Proc Natl Acad Sci U S A. 2006; 103:7142–7147. [PubMed: 16636275]
53. Nunomura A, Perry G, Aliev G, Hirai K, Takeda A, Balraj EK, Jones PK, Ghanbari H, Wataya T, Shimohama S, Chiba S, Atwood CS, Petersen RB, Smith MA. Oxidative damage is the earliest event in Alzheimer disease. Journal of neuropathology and experimental neurology. 2001; 60:759–767. [PubMed: 11487050]
54. Rakhit R, Cunningham P, Furtos-Matei A, Dahan S, Qi X-F, Crow JP, Cashman NR, Kondejewski LH, Chakrabartty A. Oxidation-induced misfolding and aggregation of superoxide dismutase and its implications for amyotrophic lateral sclerosis. J Biol Chem. 2002; 277:47551–47556. [PubMed: 12356748]

Highlights

- Ascorbate/Cu(II) mediates cleavage of bSOD1 distinct from peroxide-mediated cleavage.
- Ascorbate/ Cu(II)-mediated specific cleavage of bSOD1 is inhibited by Fe(II).
- Mass spectrometry analyses demonstrated a novel peptide bond cleavage at Gly31.
- A new His-19 coordinated binding site is proposed for exogenous copper.

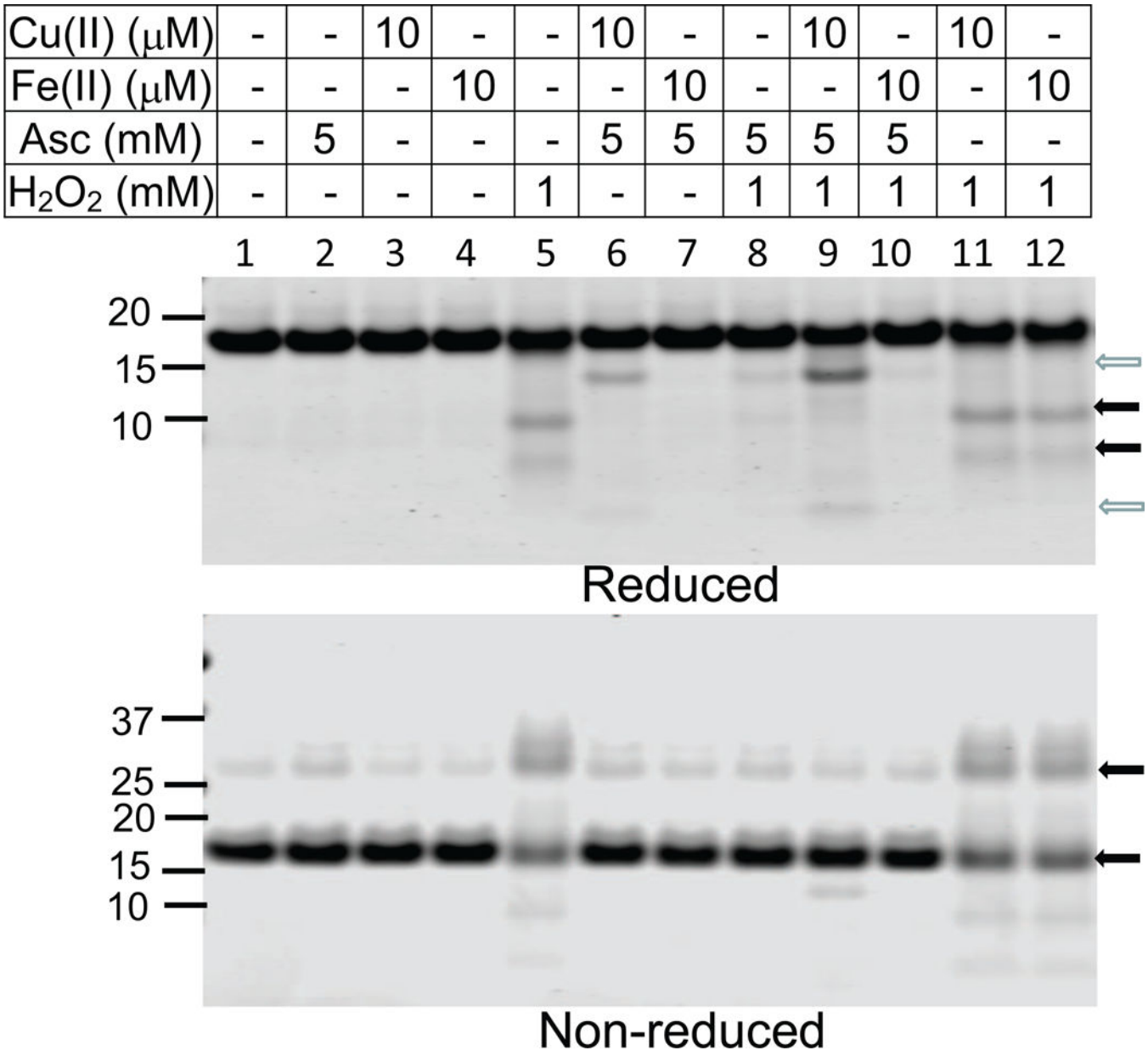

Figure 1.

Unique fragmentation of bSOD1 mediated by Asc/Cu(II).

Asc/H_2O_2 cleaves bSOD1 into 12.5 and 3.1 kDa fragments indicated by open arrows. A 3.2 μg aliquot of bSOD1 (final concentration 10 μM in 10μl reaction mixture) was incubated in 10 mM Tris-HCl, pH 7.6 with indicated concentration of sodium-ascorbate (the pH of the stock solution was ~7.4), hydrogen peroxide or Fe(II) alone or combination for 30 minutes at 37°C with Fe(II) or Cu(II) added first followed by Asc and lastly H_2O_2. After the incubation, 1.6 μg of the mix was reduced with 50mM DTT, separated by 4–12% Bis-Tris NuPAGE and stained with CBB (upper panel). Equal amounts of non-reduced bSOD1 mix were analyzed under identical conditions (lower panel). The numbers on the left of the gel

indicate MW (kDa). Two major fragments (9.5 and 6.5 kDa) generated by H_2O_2 treatment are indicated by solid arrows).

A

Asc(mM)	5	5	5	-	-	-	-	-	-	-	-
H_2O_2(mM)	1	1	1	0.1	0.3	1	3	1	1	1	1
Cu(II) (mM)	30	30	130	-	-	-	-	10	-	130	-
Fe(II) (mM)	-	-	-	-	-	-	-	-	10	-	130
DTPA(mM)	-	100	100	-	-	-	-	100	100	100	100

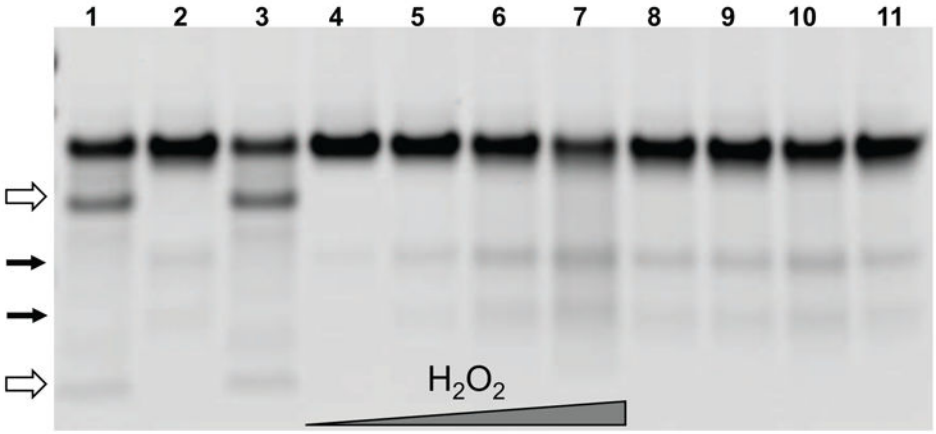

B

Asc(mM)	-	5	20	100	5	5	5	5	5	5	5	5	20	100	5	5
H_2O_2(mM)	-	-	-	-	-	-	-	0.1	0.3	1	3	1	1	1	1	1
Cu(II)(μM)	-	-	-	-	10	30	100	-	-	-	-	10	10	10	30	100

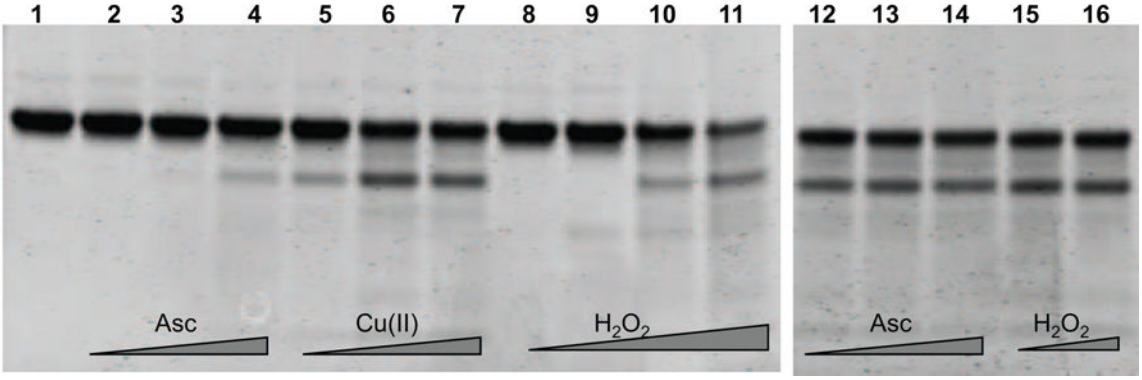

Figure 2.

Comparation of Asc and H_2O_2 mediated fragmentation of bSOD1.

A. Asc/H_2O_2 mediated fragmentation is dependent on the presence of Cu(II) ion. H_2O_2 mediated fragmentation is independent of exogenously added metal ion. DTPA was first added to bSOD1 (final 8μM), incubated for 5 minutes at 23°C and followed by addition of the indicated concentration of Asc, H_2O_2, or metal ions added in this order The resultant bSOD1 samples were analyzed under reducing conditions.

B. Titration of Asc, H_2O_2 and Cu(II) ion in bSOD1 fragmentation that generates 9.5 and 3.1 kDa fragments. bSOD1 (final 8uM) was treated with varied concentration of Asc, H_2O_2, or Cu(II) and the effect on the extent of fragmentation was assessed. The order of addition of Asc, H_2O_2, and Cu(II) was the same as described for Fig. 2A

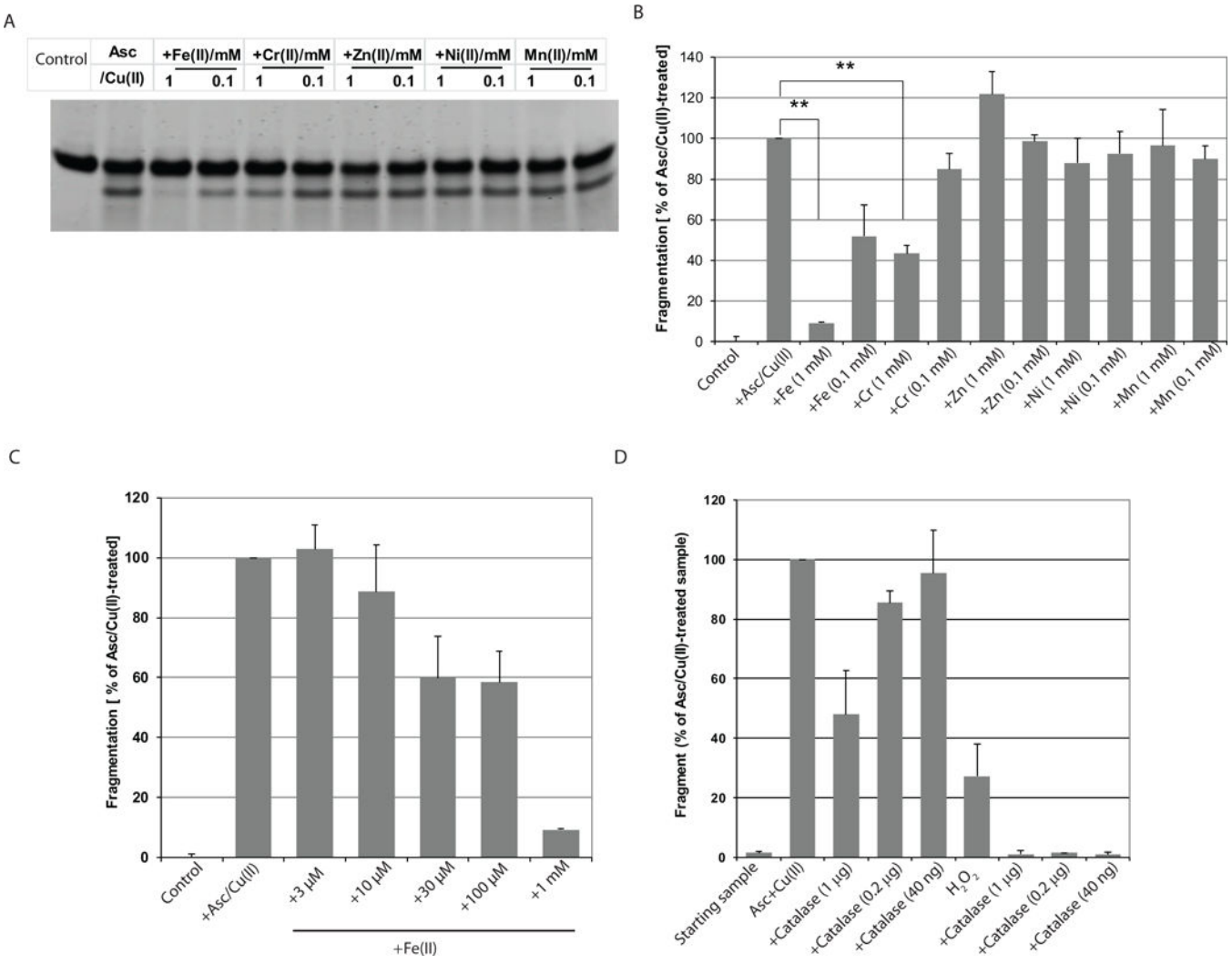

Figure 3.

Inhibition of bSOD1 fragmentation by transition metals and catalase.

A. Inhibition of Asc/Cu(II) mediated bSOD1 fragmentation by the presence of transition metals. 1 mM or 0.1 mM of transition metals were added to bSOD1 in 10 mM Tris-HCl buffer, incubated for 5 minutes at 23°C prior to the addition of 30 µM of Cu(II) and 5 mM Asc (added in this order). After incubation for 30 minutes at 37°C, the bSOD1 fragmentation was assessed by CBB staining of NuPAGE-separated samples. The sample in lane 2 is bSOD1 treated with 5 mM AsC and 30 µM Cu(II) without other transition metals.

B. Quantitation of the inhibitory effect of transition metals on Asc/Cu(II)-mediated bSOD1 fragmentation. The Y axis represents the band intensity of the 12.5 kDa fragment in each sample normalized with that obtained from Asc/Cu(II)-only treatment of the protein. The data are average of two independent experiments. **p<0.01

C. Inhibition of Asc/Cu(II) mediated fragmentation by presence of various concentrations of Fe(II). The figure represents an average of three independent experiments.

D. The Asc/Cu(II)-mediated fragmentation is not inhibited by catalase. The indicated amount of catalase was added to each reaction and incubated for 5 minutes prior to the

addition of Asc and Cu(II). The Y axis represents the relative level of the 12.5 kDa fragment to the 15.5 kDa non-cleaved bSOD1 product for each Asc/Cu(II)-treated sample. For H_2O_2 mediated fragmentation, the ratio represents the 9.5 kDa fragment to the 15.5 kDa non-cleaved product. Each reaction contains 2.6 μg bSOD1 (8μM).

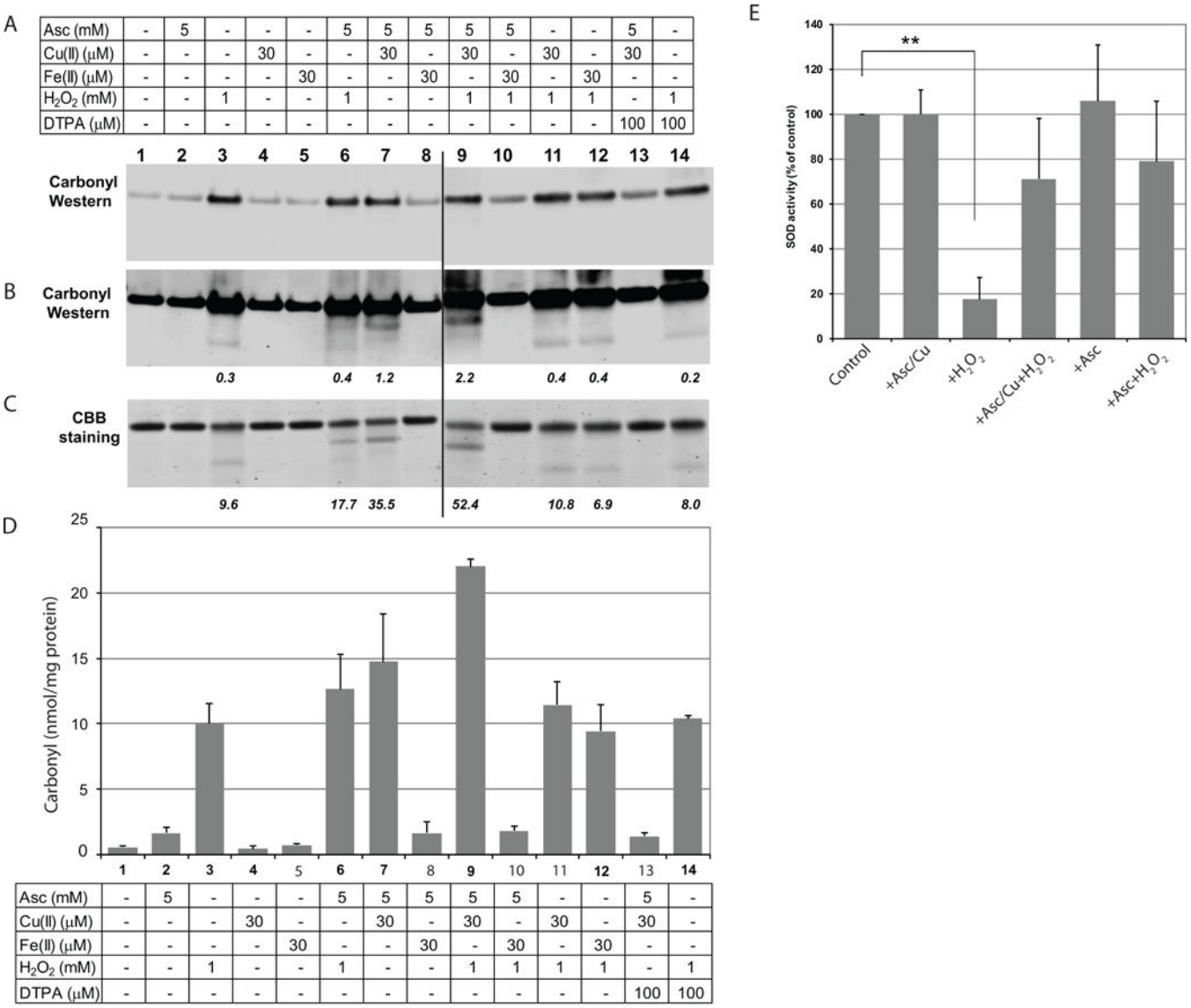

Figure 4.

Asc/Cu(II) and H_2O_2 mediated bSOD1 carbonylation and its enzymatic activity.

A. Western blot immunodetection of carbonylation. Quantitation of carbonyl moiety associated with non-cleaved and fragments of bSOD1 treated with Asc/Cu(II) or with H_2O_2. 0.4μg of treated and control bSOD1 were subjected to western blot detection of dinitrophenyl-derivatized carbonyl. DTPA was added 5 minutes prior to the addition of Asc, H_2O_2, and Cu(II) or Fe(II) that were added in this order.

B. Identical to blot A, but enhanced for brightness and contrast to show the low levels of carbonylation associated with the 12.5 and 9.6 kDa fragments. The numbers under the blot indicate the intensity of the 12.5 or 9.5 kDa fragments relative to the corresponding band for the non-cleaved intact bSOD1 in each reaction.

C. Coomassie Brilliant Blue staining of the same samples. The numbers under the image indicate the densitometric intensity of the fragment in each preparation relative to full non-cleaved bSOD1.

D. Quantitation of carbonyl in each bSOD1 preparation determined by carbonyl-ELISA. The data represent an average of two independent experiments.

E. Asc/Cu treatment does not inactivate bSOD1.

bSOD1 was incubated with 5 mM Asc/30 μM Cu(II) or 1 mM H_2O_2 as indicated in the figure for 30 minutes at 37°C and the remaining superoxide activity was determined. The data represent an average of 3–4 independent experiments. **p<0.01

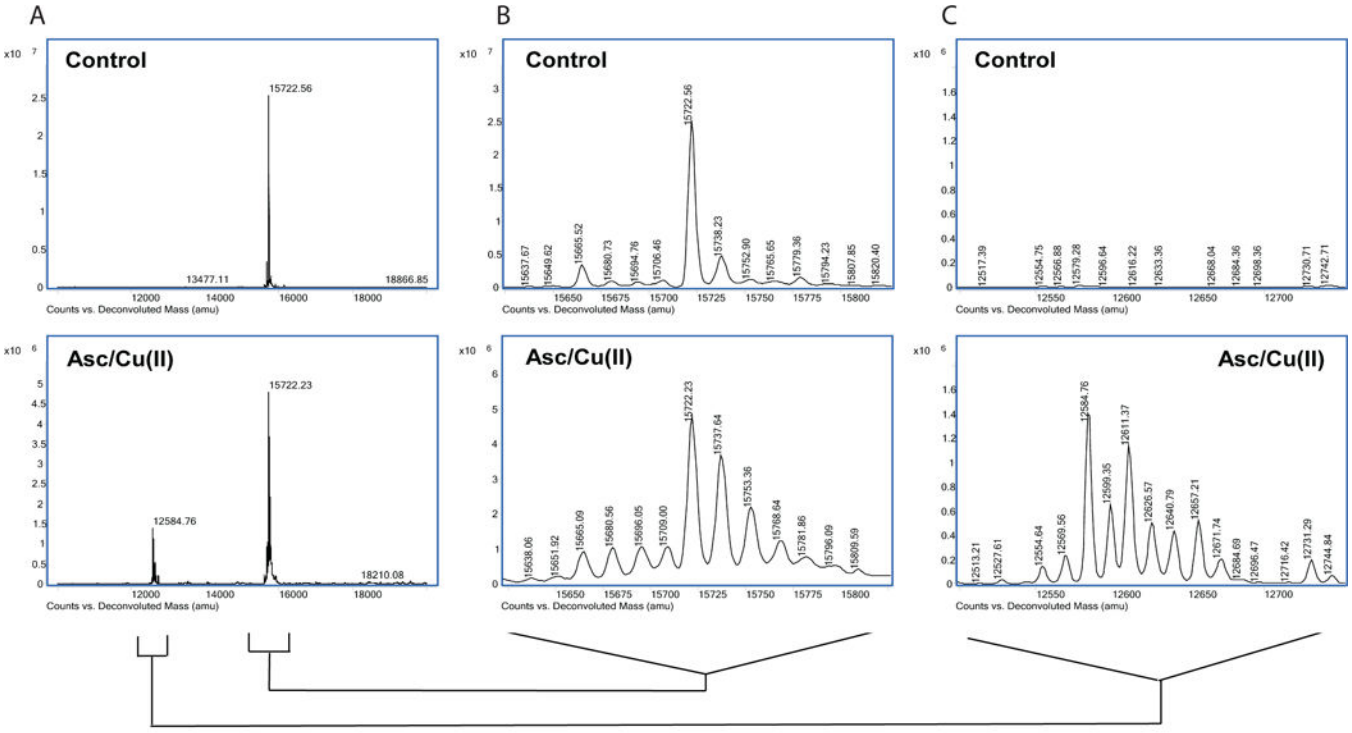

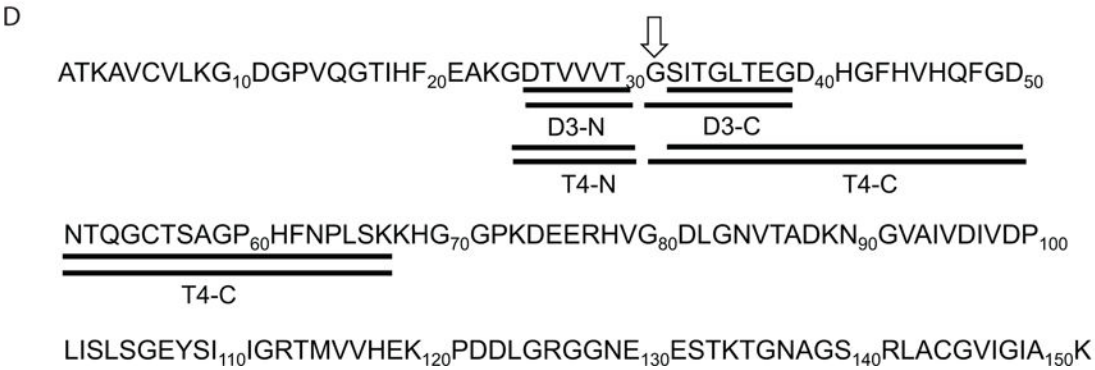

Figure 5.

Identification of the cleavage site(s) on Asc/Cu(II)-treated bSOD1

A–C. Deconvoluted intact protein mass spectra of control (upper row) and Asc/Cu(II) treated (lower row) and reduced and alkylated bSOD1. The spectra in column B and C provide expanded view of mass range 15,625–15,825 and 12,540–12,700 Da in column A, respectively, demonstrating multiple mass peaks resulted from oxidative modification and specific fragmentation by the treatment.

D. Potential tryptic and Asp-N peptides that are generated from bSOD1 fragments cleaved through diamide or α-amidation pathways at Gly31. The underline indicates tryptic or Asp-N peptides. The cleavage at Gly31 (white arrow) generates T4-N and T4-C from T4 and D3-N and D3-C from the D3 fragment (see Supplementary Fig. S1). The terminal modification in each fragment is described in the Results and Discussion.

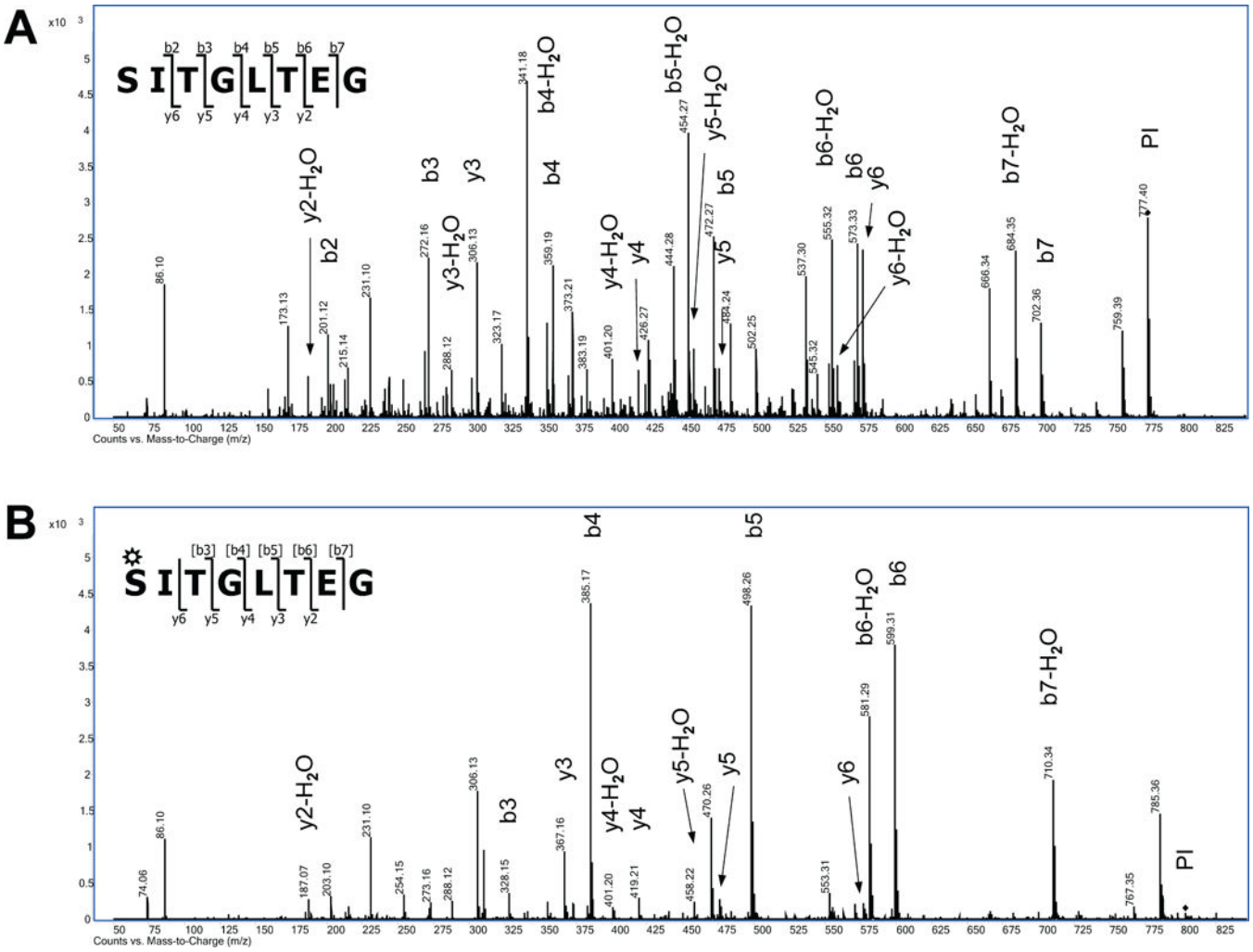

Figure 6.

Tandem MS identification of D3-C peptides generated by the cleavage of bSOD1 through diamide pathway.

Tandem MS spectrum of D3-C Asp-N peptide without (A) or with (B) N-terminus Ser isocyanation was obtained through targeting the Parent Ion (PI) of 777.3991 Da (z=1) and 803.3776 Da (z=1), respectively. The [b] ions were assigned assuming a +25.9793 mass shift on the N-terminus Ser, marked as *****S, due to the isocyanate moiety.

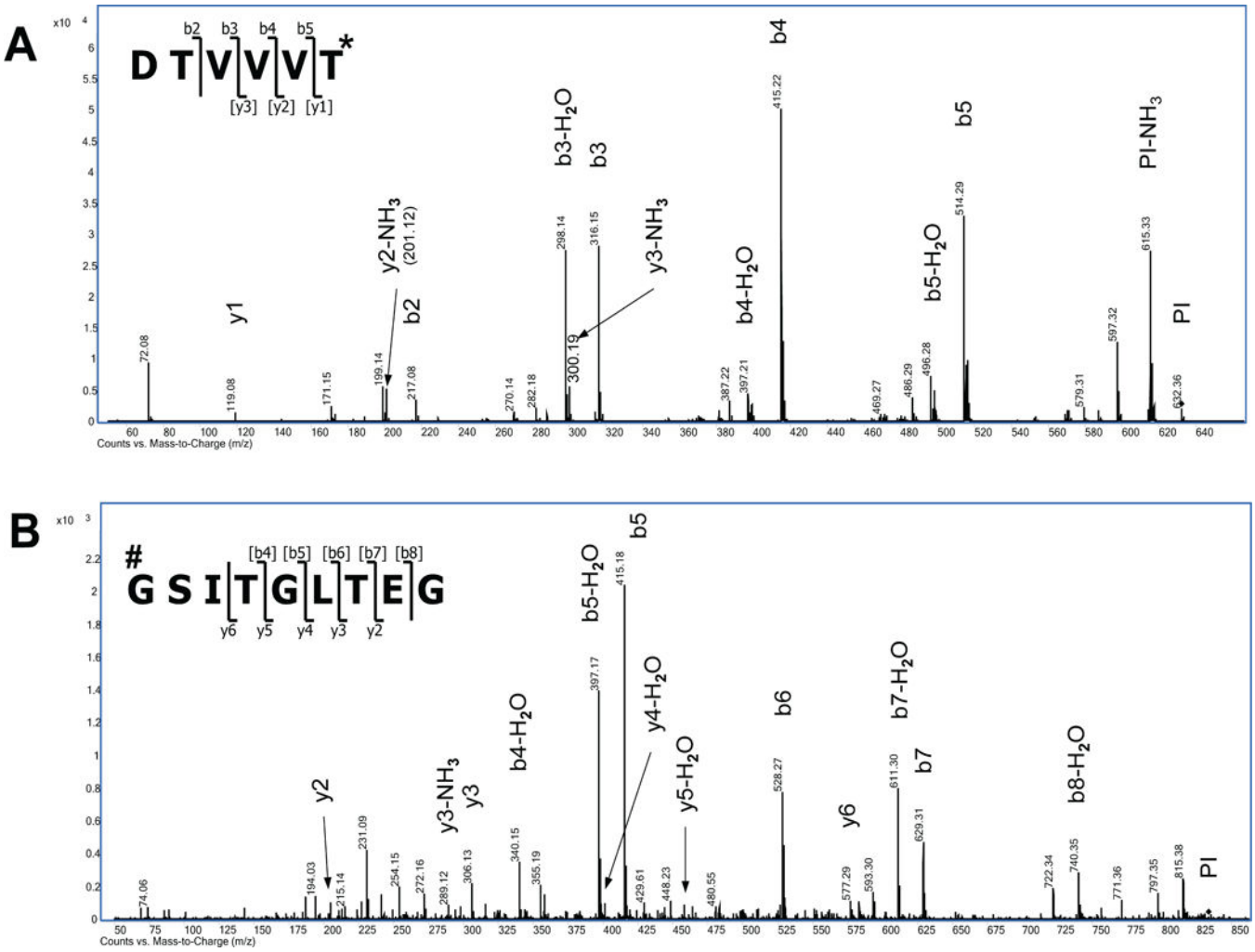

Figure 7.

Tandem MS identification of D3-N and D3-C peptides generated by the cleavage of bSOD1 through α-amidation pathway.

Tandem MS spectrum of D3-N (A) and D3-C (B) Asp-N peptide was obtained by targeting the PI of 632.3623 Da (z=1) and 833.3883 Da (z=1), respectively. The [y] ions were assigned assuming the C-terminus T* is an amide derivative of Thr with a mass shift of −0.9840, while the [b] ions were assigned based on the assumption that the N-terminus $G^{\#}$ is an α-ketoacyl-derivative of Gly with a mass shift of −1.0316 Da.

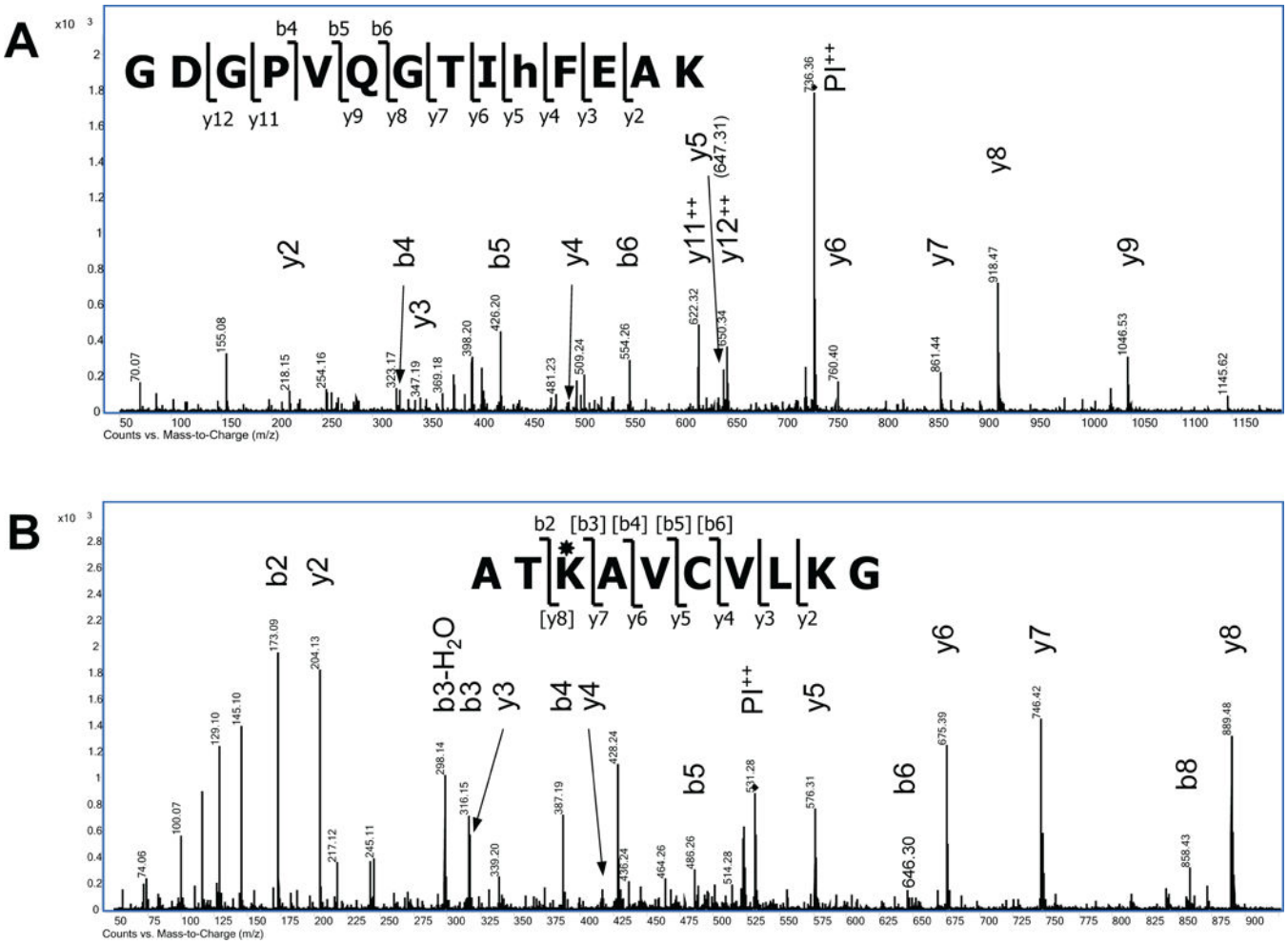

Figure 8. Tandem MS identification of Asc/Cu(II) specific novel modifications as a consequence of Cu binding to new metal binding site

(A) Identification of oxoHis-19 (h) on a tryptic peptide Gly10-Lys23 from Asc/Cu(II)-treated bSOD1 by data-dependent tandem MS. (**B**) Identification of oxidized Lys-3 (K*, delta-hydroxy-allysine) on a Asp-N peptide Ala1-Gly10 from Asc/Cu(II)-treated bSOD1 by targeting the PI of 531.2870 Da (z=2). The [b] and [y] ions were assigned assuming a +14.9633 Da mass shift at Lys3 due to the delta-hydroxy-allysine moiety.

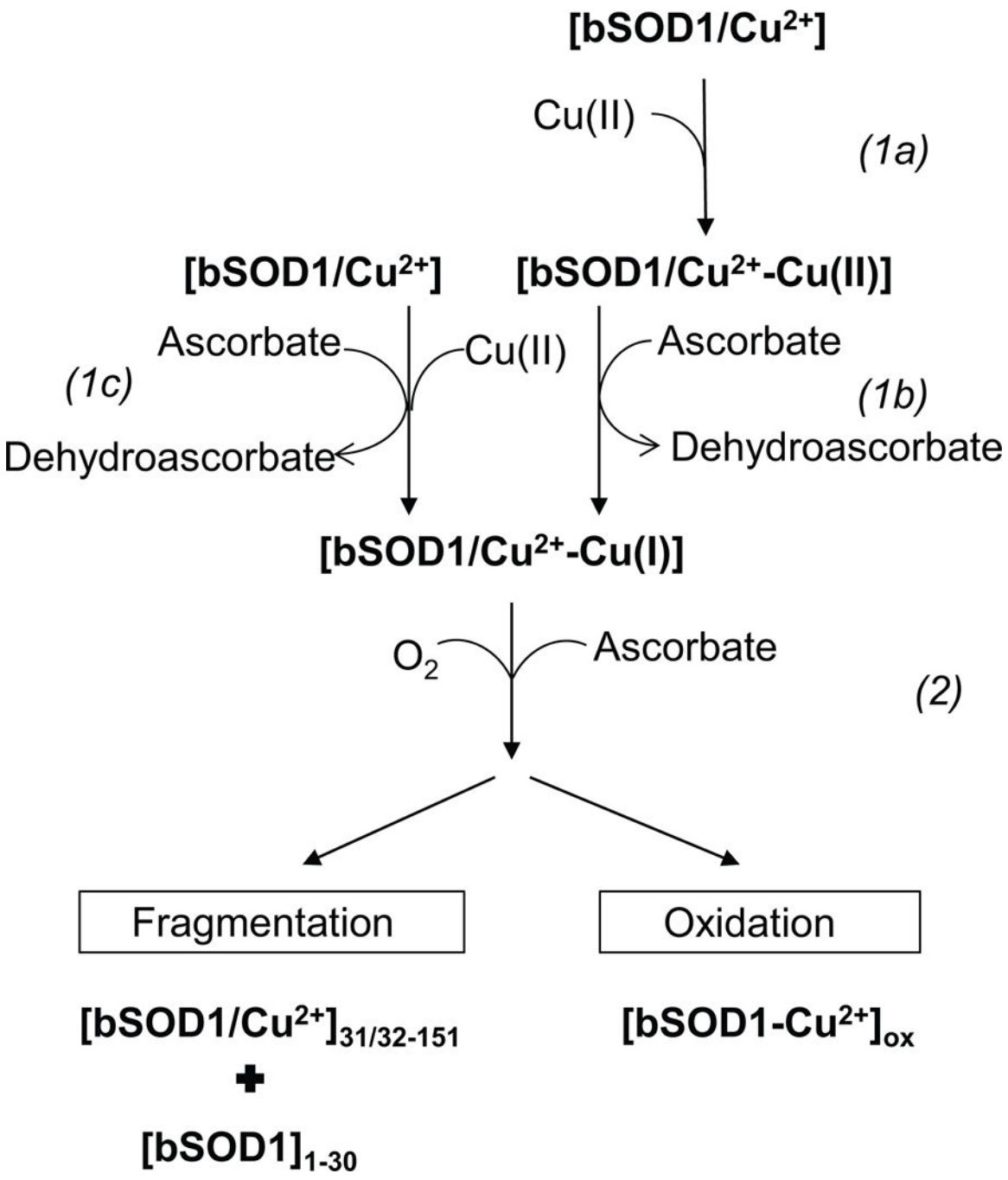

Figure 9.

Proposed biochemical mechanism underlying Asc/Cu(II) mediated bSOD1 fragmentation. In one scenario, Cu(II) binds to the bSOD1 (1a), which is then reduced to Cu(I) by ascorbate(1b). In a second scenario, Cu(II) is reduced to Cu(I) by ascorbate in aquous phase, and then binds to SOD1 (1c). Cu(II) copper ion bound to catalytic site; Cu(II), copper ion bound to surface of bSOD1; AH-, ascorbic acid; AH, semidehydroascorbate; A, dehydroascorbate. Oxidation refers to oxidation of slide chains and Fragmentation refers to peptide bond cleavage.

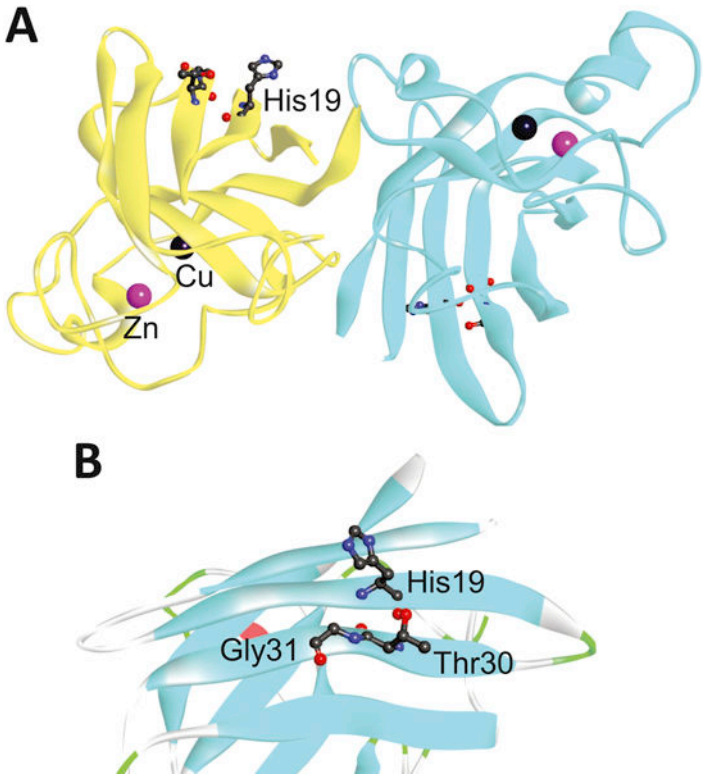

Figure 10.

3–D structure of bSOD1 with proposed new copper binding site. The images were created with the program Discovery Studio 3.1 Visualizer (Accelrys) using PDB structure entry 1Q0E (DOI: 10.2210/pdb1q0e/pdb).

A. Three dimensional structure of bSOD1 homodimer showing the relative location of catalytic copper ion and the putative copper coordinating amino acid residues. Dark blue sphere; catalytic copper ion, pink sphere; zinc ion.

B. Enlarged three dimensional structure around Thr30-Gly31-Ser32 and His19 indicating close proximity (5 Angstroms) between imidazole ring of His and α-carbon of Gly31, the presumptive target amino acid of the carbon centered hydroxyl radical.

Table 1

Potential tryptic and Asp-N peptide and identification of compounds and their molecular mass observed by LC-Q-TOF-MS peptide mapping of Asc/Cu(II) treated bSOD1

Enzyme		Potential Peptide	Mol Mass Calculated	Compound Mol Mass Observed
Trypsin	T4-N[X]	G24-T30-amide derivative	688.36	688.37
	T4-C[Y]	N-α-ketoacyl-G31-K67	3905.77	3905.74
	T4-N	G24-T30	689.36	689.37
	T4-C	S32-K67	3849.76	3849.76
	T4-C[Z]	isocyanate-S32-K67	3875.75	3875.73
Asp-N	D3-N[X]	D25-T30-amide derivative	631.34	631.35
	D3-C[Y]	N-α-ketoacyl-G31-G39	832.41	832.39
	D3-N	D25-T30	632.34	632.39
	D3-C	S32-G39	776.39	776.39
	D3-C[Z]	isocyanate-S32-G39	802.40	802.37

[X]The C-terminus amino acid of this peptide is an amide derivative

[Y]The N-terminus amino acid is a N-α-ketoacyl derivative

[Z]The N-terminus amino acid is an isocyanate derivative

Note: T4-N[X] and T4-N and D3-N[X] and D3-N were indistinguishable as the molecular mass difference between them is 1 Da which coincides with the difference of ^{12}C and ^{13}C isotope.